



ISSN: 0067-2904

Pulsed Laser Deposition of TiO₂ Nanostructures for Verify the Linear and Non-Linear Optical Characteristics

Falah A-H. Mutlak¹, Raied K Jamal*¹, Ala F. Ahmed²

¹Department of Physics, College of Science, University of Baghdad, Baghdad, Iraq

²Department of Astronomy and Space, College of Science, University of Baghdad, Baghdad, Iraq

Received: 26/9/2020

Accepted: 19/1/2021

Abstract

The present work aims to achieve pulsed laser deposition of TiO₂ nanostructures and investigate their nonlinear properties using z-scan technique. The second harmonic Q-switched Nd: YAG laser at repetition rate of 1Hz and wavelength of 532 nm with three different laser fluencies in the range of 0.77-1.1 J/cm² was utilized to irradiate the TiO₂ target. The products of laser-induced plasma were characterized by utilizing UV-Vis absorption spectroscopy, x-ray diffraction (XRD), atomic force Microscope (AFM), and Fourier transform infrared (FTIR). A reasonable agreement was found among the data obtained using X-Ray diffraction, UV-Vis and Raman spectroscopy. The XRD results showed that the prepared TiO₂ thin films were all crystallite structure with no impurity peaks of other elements. Also, their peak intensities were increased with increasing the ablating laser fluency. AFM measurements indicated that, during pulsed laser deposition, as the laser fluency was increased, the average diameter of the prepared TiO₂ nanoparticles (TiO₂ NPs) was decreased from 86 to 57 nm, although the differences were increased with the increase in the laser fluency. The multiphoton absorption was investigated using ultra-fast femtosecond laser with the z-scan method. The impact of thickness of the prepared films on the non-linear absorption coefficient was studied as well.

Keywords: ultrafast laser; femtosecond; z-scan technique; pulsed laser deposition; nanostructure.

الترسيب بالليزر النبضي للتركيب النانوي لثنائي اوكسيد التيتانيوم للتحقق من الخصائص البصرية الخطية واللاخطية

فلاح عبد الحسن مطلق¹، رائد كامل جمال*¹، الاء فاضل احمد²

¹ قسم الفيزياء، كلية العلوم، جامعة بغداد، بغداد، العراق

² قسم الفلك والفضاء، كلية العلوم، جامعة بغداد، بغداد، العراق

الخلاصة

يهدف العمل الحالي إلى تحقيق الترسيب النبضي لليزر TiO₂ والبنى النانوية والتحقق في الخصائص غير الخطية باستخدام تقنية المسح الضوئي Z، بينما التوافقي الثاني المتعلق بليزر Q-switched Nd: YAG بمعدل تكرار يبلغ 1 هرتز وطول موجي 532 نانومتر مع بثلاث نبضات ليزرية مختلفة في حدود 0.77-1.1 جول / سم² لإشعاع هدف TiO₂. تم تمييز منتجات البلازما المستحثة بالليزر باستخدام التحليل الطيفي لامتناص UV-Vis، وحيود الأشعة السينية (XRD)، ومجهر القوة الذرية (AFM)، وتحويل

*Email: raiedkamel@yahoo.com

فورييه للأشعة تحت الحمراء (FTIR). تم العثور على اتفاق معقول مع البيانات التي تم الحصول عليها باستخدام حيود الأشعة السينية و UV-Vis و Raman الطيفي. أظهرت نتائج XRD أن أغشية TiO_2 الرقيقة المحضرة كانت كلها ذات بنية بلورية مع عدم وجود قمم شوائب للعناصر الأخرى. أيضا ، زادت شدة الذروة مع زيادة فلور الليزر. أشارت قياسات AFM إلى أنه في ترسيب الليزر النبضي ، مع زيادة تدفق الليزر ، ينخفض متوسط قطر TiO_2 NPs المحضرة من 86 إلى 57 نانومتر ، على الرغم من أن الاختلافات تزداد عندما يزداد تدفق الليزر. تم فحص امتصاص متعدد الفوتونات باستخدام ليزر الفيمتوثانية فائق السرعة بطريقة المسح Z ودراسة تأثير سماكة الأغشية المحضرة على معامل الامتصاص اللاخطي.

Introduction

Titanium dioxide (TiO_2) is an important material for many physical applications, including solar cells [1] and heterogeneous catalysis [2-6]. Generally, TiO_2 was applied in two major forms, namely thin and powder films. The former TiO_2 form was majorly utilized for liquid and gas phase catalysis. Normally, its photocatalytic activity was specified via particle size, phase composition [7], and the position of valance and conduction bands in the energy scale [8]. More recently, TiO_2 was utilized in photovoltaic applications, including photoelectron chemical systems as well as the dye-sensitized solar cells for the harvesting of photons [9]. Also, TiO_2 in such form is offering energy alignments between energy positions of valance band edge and the redox species in electrolyte, through possible biasing photoanodes. Several deposition approaches of TiO_2 thin films were employed, such as metal organic chemical vapor deposition [10], reactive RF sputtering [11], direct current (DC) magnetron sputtering [12], and sol-gel spin-coating [13]. Currently, laser has various applications, one of which being the thin film preparation field which is referred to as pulsed laser deposition (PLD) [14-16], along with other technique used for other applications [17-18]. With such an approach, the thin films were prepared through ablation of at least one of the targets illuminated through focused pulsed laser beam. In 1965, Smith and Turner initially utilized this approach [19] to prepare semiconductors in addition to dielectric thin films. Moreover, is the approach was developed through the study of Dijkkamp and colleagues in 1987, who described superconductors of high temperature. Their study indicated major laser induced plasma LIP characteristics, particularly the stoichiometry transfer between deposited and target films, the elevated deposition rate of approximately 0.10 nm for each pulse, and the occurrence of droplets on substrate surface. The benefit of utilizing PLD, as compared to other techniques of sputtering, is its efficiency and simplicity in producing multi-layered films of a variety of materials through sequential ablation of assorted targets. The thickness of the thin film is controlled by the number of pulses of the laser used, down to the single atom layer. One of the major PLD features is that the target stoichiometry might be retained in the deposited film, while PLD has also some drawbacks. In the present study, TiO_2 thin films with nanostructure were fabricated through the PLD approach which is commonly utilized for oxide film growth since it allows the stoichiometry of the synthesized material. Also, the structural and optical characteristics of TiO_2 thin film were examined.

Experimental Part

Turner and Smith initially utilized the general typical setup for pulsed laser deposition [19]. In the present work, TiO_2 was utilized as a target, with 2cm diameter and 1cm thickness, and fixed the target at the top chamber. The glass substrate was applied as one of the substrate materials for studying the non-linear and linear characteristics. Substrate cleaning was required for ensuring a surface that is free from contamination films, including absorbed water. Also, the glass substrates were cut into standard sizes (10x10) mm, cleaned ultrasonically in acetone, and then left the glass substrate in an oven to dry. In addition, the effect of laser fluencies of 0.77, 0.91 and 1.1 J /cm² on optical and structural characteristics of TiO_2 thin films was examined. Titanium dioxide thin films were grown for 5mins on a glass substrate, while the chamber's base pressure was 2.0×10^{-5} mbar. LIP is a method of high importance for metal as well as semiconductor deposition, offering uniform coverage, high deposition rate, and dc magnetron sputtering, ultimately providing the capability for rapidly depositing large amounts of material. In the present work, several characterization approaches were utilized for evaluating the structural and optical characteristics of TiO_2 thin films. For the purpose of avoiding fast drilling, the target was mounted on a rotating holder located at a distance of 45 mm from the substrate for improving the film's uniformity.

For the purpose of determining the TiO₂ film thickness, the optical interference fringes measurement was utilized, which is non-destructive, precise and rapid. XRD is applied for determining the overall structure of TiO₂ thin films, involving polycrystals orientation, unknown materials grain size, lattice constants, and single crystals orientation. In the current work, the thin films were studied via XRD with Cu-K α X-ray tube ($\lambda = 0.154056 \text{ \AA}$). Also, the XRD spectrum was achieved at diffraction angle values 2θ , ranging 10° - 60° .

The optical measurements of TiO₂ thin films were achieved by utilizing a U.V. mate SP8001 double beam spectrophotometer (Metertech Corporation, Taipei, Taiwan) that covers wavelength values in the range of 190-1100nm. In addition, the investigation of the non-linear absorption at near resonant regime was conducted utilizing a fully-computerized, single beam, open aperture z-scan femtosecond laser [18]. Femtosecond laser with 100fs and 80 mJ/cm² maximum laser fluencies was utilized as a laser source, while pulse duration was estimated via auto-correlation system. Energy was estimated via pyroelectric energy probe (PDA-36A, Thorlabs) which covers a range of 350-1000nm. Beam profile was adjusted through a spatial filter with a beam quality of $M^2 \approx 1.7$. A convex lens with a focal length of 15 cm was used to produce a waist of 37 μm . The sample was moved along the beam axis (z-axis) via a Rayleigh distance of 2.1mm.

Results and discussion

The PLD is a technique of high importance for synthesizing nanostructured TiO₂ because of the contactless treatment. Nanostructures of various patterns might simply be achieved on treated surfaces with no more masking. The thin films' thickness, which was found via optical interference approach, showed values of 200, 250, and 300 nm. XRD is a convenient method for determining the structure and crystallite size of nanostructures. Figure-1 shows the XRD pattern of the TiO₂ nanostructures prepared by LIP. The XRD pattern exhibits peaks centered at $2\theta = 25.5^\circ$, 38.2° , 47.3° , 54.4° and 63.6° , corresponding to (101), (112), (200), (104) and (204) planes, respectively. These planes agreed with the crystal planes that are related to TiO₂ phase, as determined based on the data published by the Joint Committee on Powder Diffraction Standards (JCPDS No 21-1272). Also, the broadening of the XRD pattern verified the reduction in the size of the generated TiO₂ nanostructures. The values of the crystallite size (D) of the synthesized sample were estimated based on Scherrer's equation shown in Table-1.

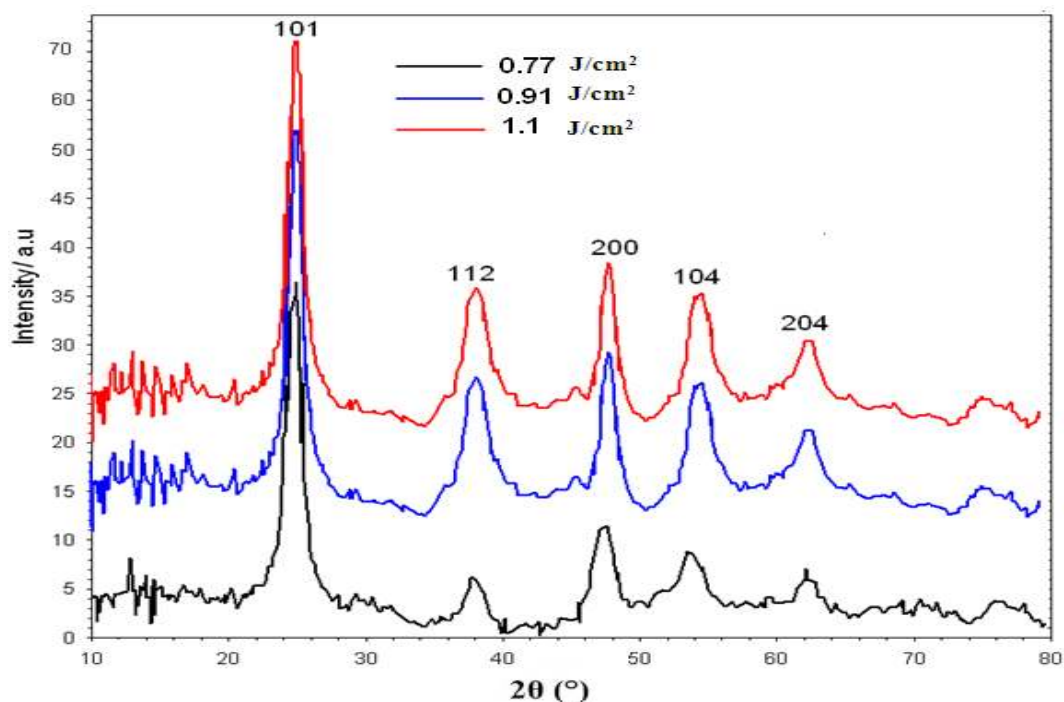


Figure 1-X-ray diffraction (XRD) of TiO₂ nanostructures prepared by laser –induced plasma at different laser fluencies.

Table 1-Structural properties of TiO₂ nanostructures at different laser fluencies

Laser fluencies J/cm ²	<i>hkl</i>	2θ	$d A^\circ$	<i>FWHM</i>	<i>D nm</i>
0.77	101	25.2	3.5	0.86	9.5
0.91	101	25.6	3.24	0.94	8.8
1.1	101	25.6	2.48	0.98	8.5

AFM measurements were carried out to investigate the morphology and size of TiO₂ nanostructures synthesized by ablating the TiO₂ metal at different laser fluencies (0.77, 0.91 and 1.1 J/cm²). As shown in Figure-2, the morphology and size of TiO₂ nanostructures varied with increasing the laser energy.

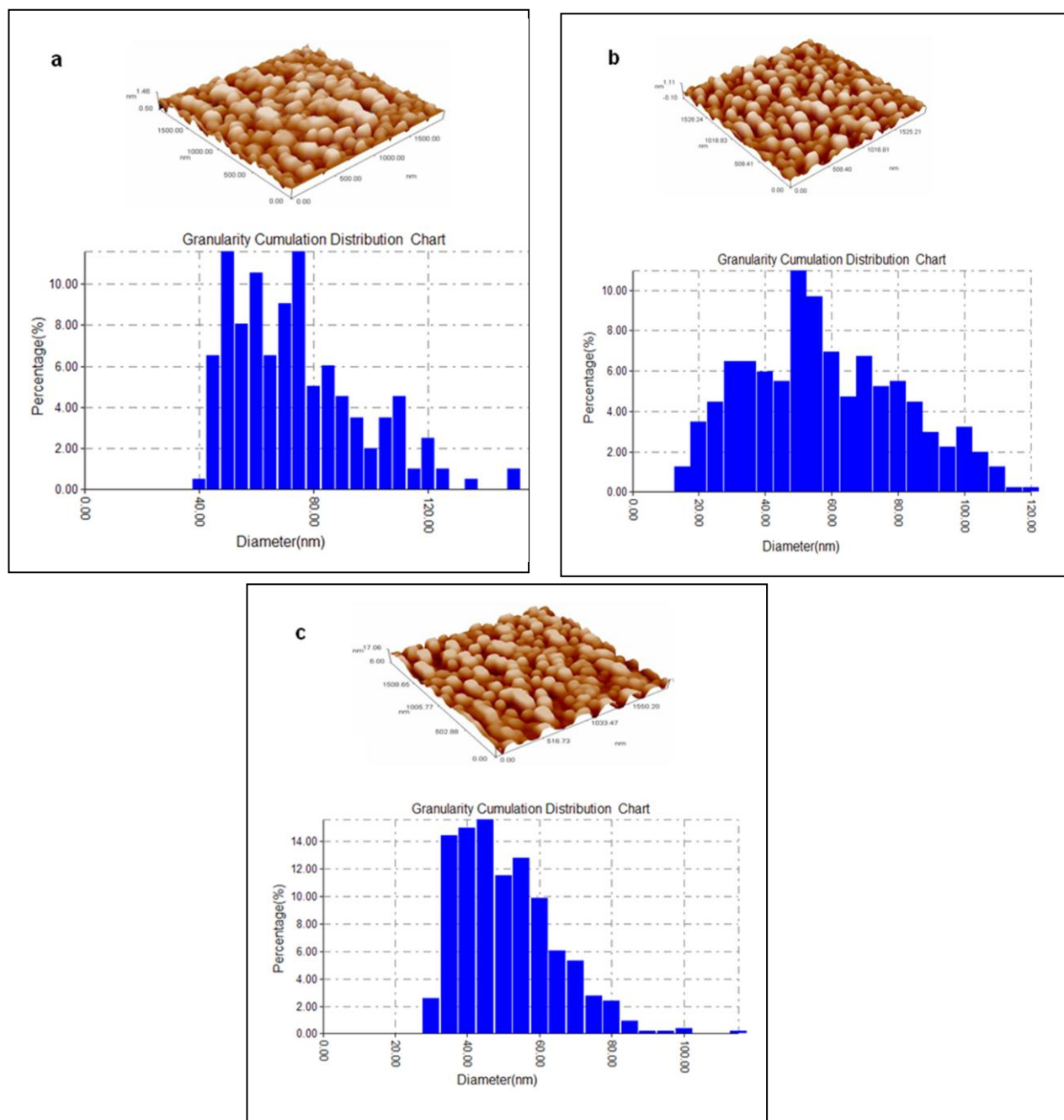


Figure 2-3D AFM images and granularity accumulation distribution chart of TiO₂ nanostructures prepared by laser –induced plasma at different laser fluencies (a) 0.77 J/cm², (b) 0.91 J/cm² and (c) 1.1 J/cm².

The average diameter size was decreased from 86 to 57 nm with increasing the laser energy. The difference in size and morphology are strongly dependent on the characteristics of the generated plasma on the surface of the target, according to the interaction of laser pulse with the solid target. At low laser energy, the plasma of low temperature and large nanoparticles size is re-produced. By increasing the energy of laser pulse, a high temperature plasma plume is generated, leading to larger kinetic energy that increases collisions among the initially-formed large nanoparticles. This effect causes a reduction in particle size and probability of adhesion and makes the size of each nanoparticle relatively uniform. Figure-2 presents the 3D AFM images of TiO₂ nanostructures prepared at different laser fluencies; (a) 0.77 J/cm², (b) 0.91 J/cm² and (c) 1.1 J/cm². SEM measurements were carried out at laser fluency equal 1.1 J/cm². The nanoparticles appeared in spherical shape and high number. In addition, some aggregations between these nanoparticles could be noted. Once the nano-colloidal solution is synthesized, the nanoparticles can be affected by the attractive Van der Waals force, which promotes the growth of nanoparticles with aggregation, as shown in Figure-3.

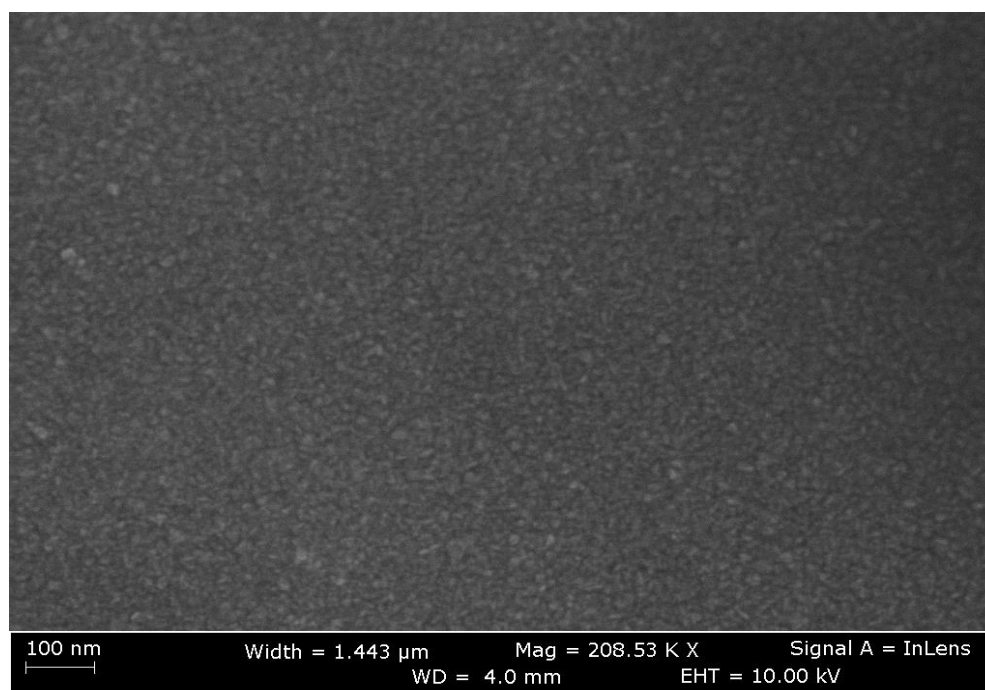


Figure 3-SEM of TiO₂ nanostructures prepared by laser –induced plasma at 1.1 J/cm² laser fluency.

The absorption spectra of the synthesized TiO₂ nanostructures were recorded in the wavelength scan region (200–1100 nm). Figure- 4 illustrates the optical absorption spectra of TiO₂ nanostructures that are prepared at different laser fluencies. A significant increase in the absorption, below 334 nm, was observed and the absorption edge was shifted toward shorter wavelengths with increasing the laser energy. Moreover, the intensity of the absorption peaks is increased with the increase in laser energy, due to the high deposition of nanoparticles. This can be explained by delivering more energy to the target, which leads to the production of intense plasma plume and the ablation of a larger amount of material so that the nanostructure becomes denser.

FTIR measurement was performed over the range of 400–4000 cm⁻¹ for the TiO₂ nanostructures to confirm the formation of oxide bonds. Figure-5 shows FTIR spectra of TiO₂ nanostructures prepared at different laser fluencies. The intense peaks centered at 480 cm⁻¹ are allocated to the bending vibration related to O-Ti-O bond. The absorption of water molecules observed as broad peaks at 3350 cm⁻¹ corresponds to the stretching vibrations of O-H bond, while the weak peaks at 1630 cm⁻¹ were a result of the bending vibration of H-O-H bond.

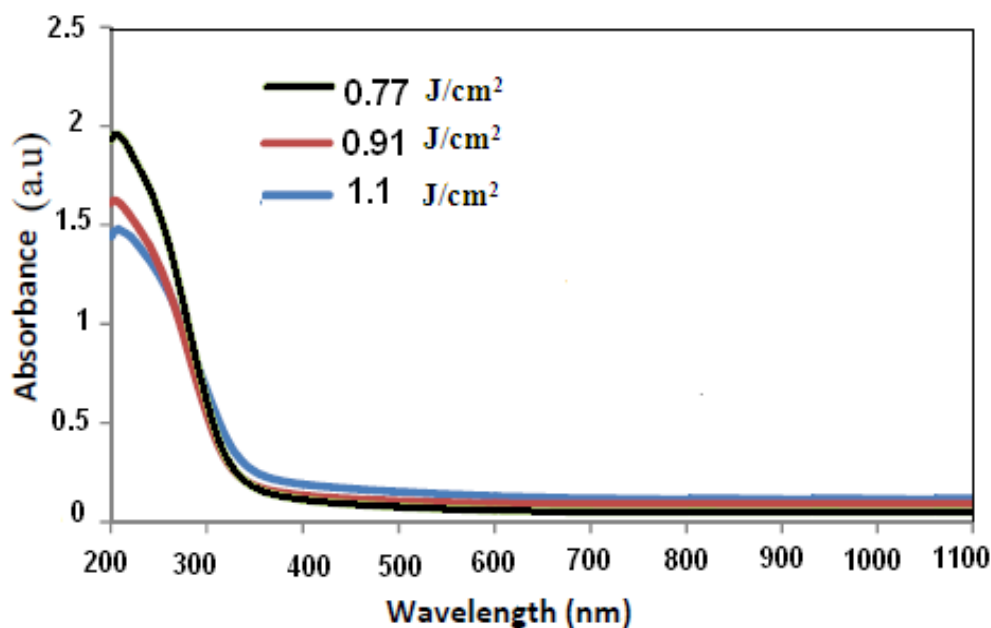


Figure 4-UV-Vis absorbance spectra of TiO₂ nanostructures prepared at different laser fluencies.

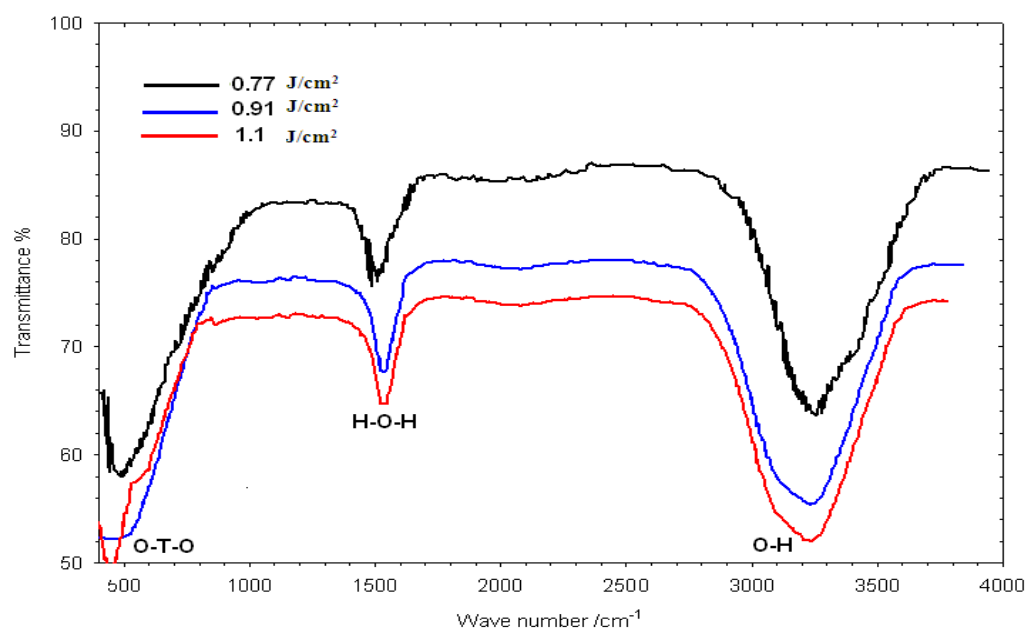


Figure 5-FTIR spectrum of TiO₂ nanostructures prepared at different laser fluencies

Results of the Raman mode of the TiO₂ samples after irradiation at different fluencies are shown in Figure-6. Raman spectra of the synthesized TiO₂ nanoparticles show that, in accordance with the XRD results, most of the crystalline phases is anatase, without appreciable amounts of rutile or brookite phases. As the crystallite size increases, the Raman blueshift and bandwidth decreases, in a total accordance with the phonon confinement model. Another possibility is to look closely at the Raman bands that appear in the low-wavenumber zone due to acoustic-phonon confinement.

Normalized energy transmittance with regard to the three photon absorption values of open aperture z-scan is provided by Sutherland *et al.* [20], as follows:

$$T(z) = \frac{1}{\pi^{0.5} P_0} \int_{-\infty}^{\infty} \ln\{[1 + P_0^2 e^{-2x}]^{0.5} + P_0^2 e^{-x^2}\} dx \quad \text{--- (1)}$$

in which $P_o = (2\gamma I_o^2 L_{eff})^{0.5}$ and $I_o = I_{o0}/(1+z^2/z_o^2)$ represent the intensity of the excitation at position z , $z_o = \pi\omega_o^2/\lambda$, where z_o represents Rayleigh's range, ω_o represents minimal waist of the beam at the focal point ($z=0$), λ represents the laser free-space wavelength, $L_{eff} = [1 - \exp(-2\alpha_o L)]/2\alpha_o$ represents the effective sample length of the 3PA procedures, L represents the length of sample, and α_o represents the coefficient of the linear absorption. In addition, the graphs of the open aperture z-scan were often normalized to linear transmittance; for instance, transmittance at high $|z|$ values. 3PA coefficient might

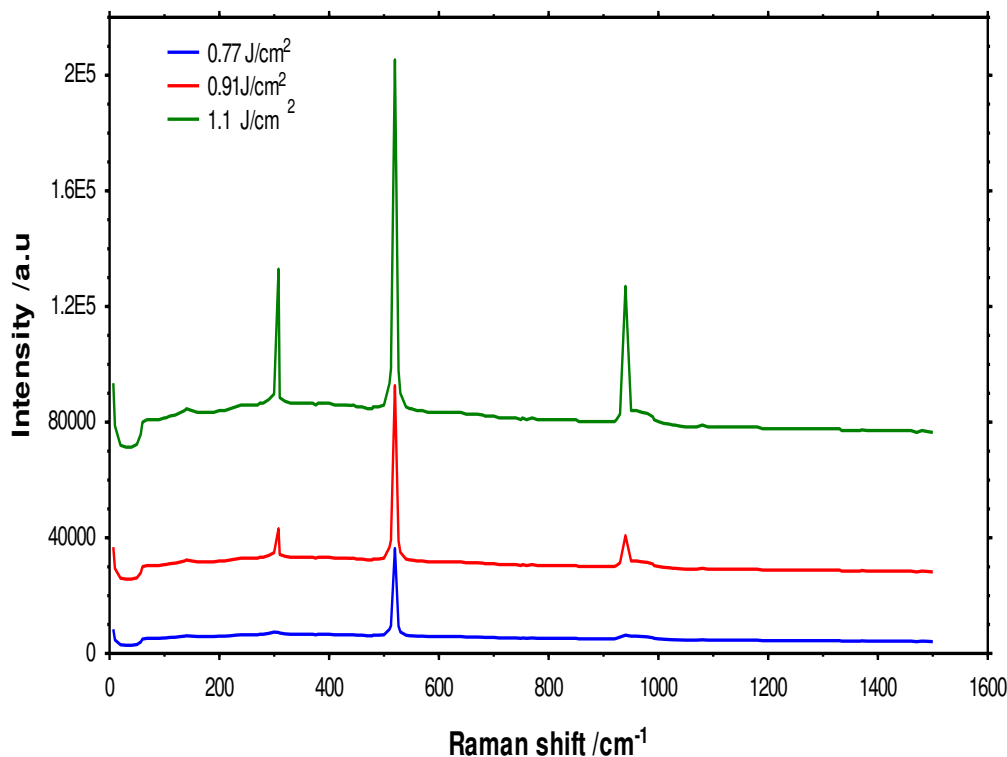


Figure 6-Raman spectra of TiO₂ nanostructures prepared at different laser fluencies.

be obtained from the optimal fit between eq2 and experiment (OA) z-scan curve. In the case when P_o is less than 1, eq2 might be expanded in Taylor series, as in the following form [20]:

$$T = \sum_{m=1}^{\infty} (-1)^{m-1} \frac{P_o^{2m-2}}{(2m-1)! (2m-1)^{0.5}} \quad \text{---(2)}$$

In the case when high order terms are ignored, the transmission as incident intensity function is provided as reported by Sutherland [20]:

$$T = 1 - \frac{\gamma I_o^2 L_{eff}}{3^{\frac{3}{2}}} \quad \text{---(3)}$$

The curves in Figure-7 were the optimal fit for eq3, which show the depth of the absorption dip as linearly proportionate to 3PA coefficient γ . Yet the trace shape was mainly specified by Rayleigh's range of focused Gauss beam.

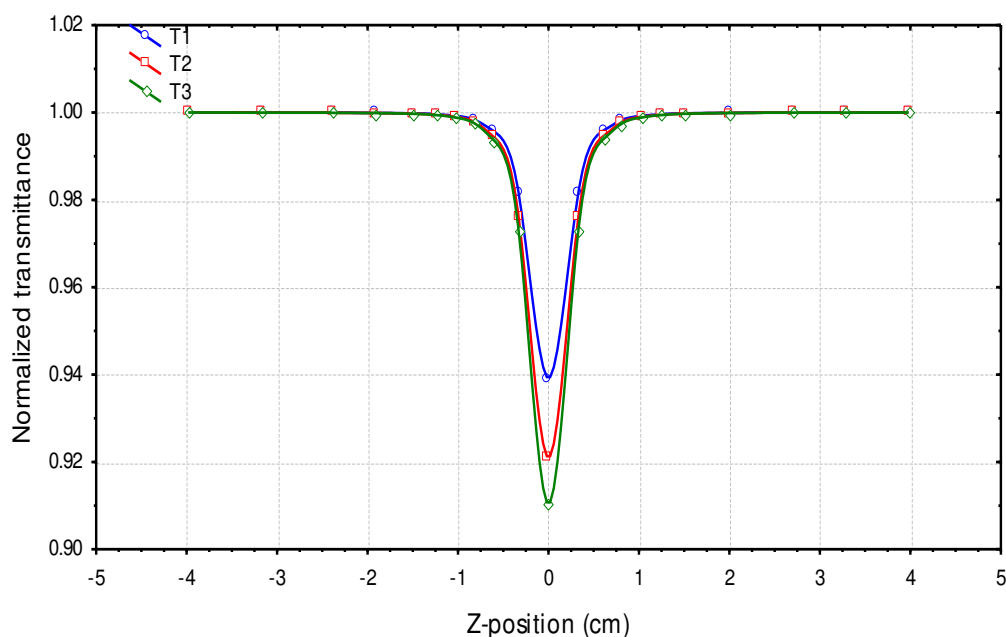


Figure 7-OA z-scan measured at a maximum influence of 80 mJ/cm^2 , wavelength of 800 nm , pulse duration of 100 fs , and repetition rate of 10 kHz . Normalized transmittance spectra of TiO_2 nanostructures were prepared at different laser fluencies.

The fitted values of γ are shown in Table -2. It is observed that when the laser fluencies increase, there will be an increase in the prepared film's thickness, and therefore the values of the effective length will increase exponentially, which leads to decreased transmittance and an increase in the non-linear absorption coefficient.

Table 2-The fitted values of γ with different laser fluencies and thickness of sample

Laser fluencies J/cm^2	$L_{\text{eff cm}}$	$\gamma \text{ cm}^3/\text{GW}^2$
0.77	0.000843	0.0586
0.91	0.00098	0.0655
1.1	0.00104	0.0780

Conclusions

Through this work, we could conclude that the three-photon absorption was observed in TiO_2 nanocrystalline prepared by pulsed laser deposition, by illuminating it with femtosecond Titanium-Sapphire laser. The laser fluencies have considerable effects on thickness of films prepared via pulsed laser deposition, which in turn will change the value of the non-linear absorption coefficient of the films prepared. The proposed synthesis method allows an easy synthesis of TiO_2 nanostructures with a controlled size (range of $86\text{-}57 \text{ nm}$), depending on the laser fluencies.

References

1. Fujishima, H., K. 1972. "Electrochemical photolysis of water at a semiconductor electrode", *Nature*, **238**(1972): 37-38.
2. Lin, H., Huang, C.P., Li, W., Ni, C., Shah, S.I. and Testing, Y.H. 2006. "size dependency of nanocrystalline TiO_2 on its optical properties and photocatalytic reactivity exemplified by 2-chlorophenol", *Applied catalysis B- Environmental*, **68**(2006): 1-11.
3. Oregan, M. Gratzel, 1991. "A low-cost, high- efficiency solar cell based on dye-sensitized colloidal TiO_2 film", *Nature*, **353**(1991): 737-740.
4. A Hagfeldt, M. Gratzel, 2000. "molecular photovoltaics", *Accounts of Chemical Research*, **33** (2000): 269-277.

5. Valden, M., Lai, X. and Goodman, D.W. **1998**. "Onset of catalytic activity of gold clusters on titania with the appearance of nonmetallic properties" *Science*, **281**(1998): 1641-1650.
6. Watanabe, T., Nakajima, A., Wang, R., Minabe, M., Koizumi, S., Fujishima, A., Hashimoto, K. **1999**. "photocatalytic activity and photoinduced hydrophilicity of titanium dioxide coated glass", *Thin Solid Film*, **351**(1999): 260-263.
7. Ding, Z., Lu, G.Q. and Greenfield, P.F. **2000**. "Role of the Crystallite Phase of TiO₂ in Heterogeneous Photocatalysis for Phenol Oxidation in Water", *Journal of Physical Chemistry B*, **104**(2000): 4815-4820.
8. Xu, Y., M. and Schoonen, M.A. **2000**. " The absolute energy position of conduction and valence bands of selected semiconducting minerals", *American Mineralogist*, **85**(2000): 543-556.
9. SKitazawa, S.I., Choi, Y., Yamamoto, S. and Yamaki, T. **2000**. "Preparation of Nanostructure TiO₂ at Different Temperatures by Pulsed Laser Deposition as Solar Cell", *Thin Solid Films*, **515**(2000): 1901-1904.
10. Rausch, N. and Burte, E.P. **1993**. "Thin TiO₂ films prepared by low pressure chemical vapor deposition", *Journal of the Electrochemical Society*, **140**(1993): 145-149.
11. Battiston, G.A., Gerbasi, R., Porchia, M. and Marigo, A. **1994**. "microstructure modification of amorphous titanium oxide thin film during annealing treatment", *Thin Solid Films*, **239**(1994): 186-191.
12. Sawicka, P. and Sibinska, M. **2019**. "characteristics of TiO₂, Cu₂O, and TiO₂/Cu₂O thin films for application in PV devices", *AIP Advances*, **9**(2019)
13. Ozer, N., Demiryont, H. and Simmons, J.H. **1991**. "optical properties of sol-gel spin-coated TiO₂ films and comparison of the properties with ion-beam-sputtered films", *Applied Optics*, **30**(1991): 3661-3666.
14. Falah A-H. Mutlak, **2014**. "Photovoltaic enhancement of Si micro-and nanostructure solar cells via ultrafast laser texturing", *Turkish J. of physics*, **38**(1): 2014.
15. Raied K. Jamal, Mohammed A. Hameed, Kadhim A. Adem, **2014**. "Optical properties of nanostructured ZnO prepared by a pulsed laser deposition technique", *Materials Letters*, **132**(2014): 31-33.
16. Raied, K. Jamal, Falah A-H. Mutlak, Fouad Tarq Ibrahim, Uday M. Nayef, **2020**. "Synthesis of Ag₂O films by pulsed laser deposited on porous silicon as gas sensor application", *Optik* **218** 164971.
17. Rosendo Valero, Ángel Morales-García and Francesc Illas, " Investigating the character of excited states in TiO₂ nanoparticles from topological descriptors: implications for photocatalysis", *Physical Chemistry Chemical Physics*, **5**(2020).
18. Mengjie, Wu. and Kun, L. **2020**. "Application of and research on TiO₂ photocatalysis technology", *E3S Web Conf.*, 165.
19. Smith, H.M. and Turner, A.F. **1965**. "Vacuum deposition thin film using a ruby laser", *Appl. Opt.* **4**: 147.
20. Sutherland, R. L., McLean, D. G. and Kirkpatrick, S. **2003**. *Handbook of Nonlinear Optics*. Second Edition. Reserved and Expanded. New York, NY: Marcel Dekker.